Optimal Active Control of a Wave Energy Converter

Edo Abraham and Eric C. Kerrigan

Abstract— **This paper investigates optimal active control schemes applied to a point absorber wave energy converter within a receding horizon fashion. A variational formulation of the power maximization problem is adapted to solve the optimal control problem. The optimal control method is shown to be of a bang-bang type for a power take-off mechanism that incorporates both linear dampers and active control elements. We also consider a direct transcription of the optimal control problem as a general nonlinear program. A variation of the projected gradient optimization scheme is formulated and shown to be feasible and computationally inexpensive compared to a standard NLP solver. Since the system model is bilinear and the cost function is non-convex quadratic, the resulting optimization problem is not a convex quadratic program. Results will be compared with an optimal command latching method to demonstrate the improvement in absorbed power. Time domain simulations are generated under irregular sea conditions.**

Index Terms— **Wave energy, Optimal control, Projected gradient method**

I. INTRODUCTION

Oscillating body wave energy converters (WECs) have a narrow bandwidth and early research attempted to use mechanical impedance matching schemes to maximize the velocity and hence the absorbed power from sinusoidal (or regular) waves [1]. Simple frequency domain analysis was used to derive optimal amplitude and phase conditions on the velocity of the device with respect to a sinusoidal wave excitation force. Often called *reactive* control in the wave energy literature [1], this method's theoretical optimal resonance condition, of having the velocity in phase with the sinusoidal force, results in unrealistically large amplitudes and large two-way energy transfers between the body and the power take-off (PTO) mechanism. This method's shortcomings include its inability to handle physical constraints [1], [2] and its non-applicability to systems with a nonlinear PTO.

In [3], only the phase criteria is met through latching control — during its oscillation, the body is latched (i.e. prevented from moving) when its velocity vanishes and released at a favorable time. In [4] an optimal sequence of latching/unlatching commands is computed to maximize extracted energy in a simplified model. Since then, optimal latching control has been widely applied to single DOFs devices [2], [5]–[7] as well as WECs with multiple DOF [6], [8], [9]. However, the effectiveness of latching diminishes for an array of devices interacting with each other; the phase condition loses meaning and optimal power absorption no more requires all bodies to have a velocity in phase with the excitation force [10]. This has motivated some research in the application of advanced optimal active control schemes to wave energy. Another passive method, called *declutching or unlatching* control [11], switches the damper PTO on-off optimally and is practically implemented using a simple by-pass valve.

The works in [12], [13] consider the use of an active force within the framework of model predictive control and so are of importance to the present article. Both papers consider only an active element for the PTO and depend on the reformulation of an energy maximization problem to discrete-time model problems. In [12], the radiation force is expressed as a linear function of the WEC velocity. Using the velocity as the optimization variable, the discretized optimization problem over a finite prediction horizon is shown to be a positive semidefinite quadratic program in the discrete velocity values – a convex problem. The emphasis in [13] is on discretizing the system using a triangle-hold such that the objective function can be approximated with one where the optimization parameters become changes in the control input at each sampling time; the method employed allows the approximation of the objective function by a semidefinite quadratic cost. Regularization terms are also added to impose penalities on the control and its derivative. However, as will be shown in this article, the optimal control is of bang-bang type when no displacement or velocity constraints are imposed or when they are inactive. This would exploit the practical advantage that bang-bang controllers can be implemented with simple on-off machinery.

In the present article, we consider a general optimal active control problem for a heaving point absorber. It is general in the sense that it considers a PTO with a controlled damping element in addition to the active control force considered by [12], [13]. As such, it reduces to an optimal declutching type problem if we remove the active control command, and it reduces to the absorbed energy maximization problems considered in [12], [13] if the damping element is removed. The result is a problem with a bilinear dynamical system and a quadratic, but non-convex, cost function, unlike the convex quadratic programs in [12], [13]. In addition to simulations as in [11], we show that the optimal controller is on-off in nature in this general PTO setting. This is done by proving that the considered optimal control problem has a bang-bang solution when only control constraints are imposed. Moreover, this formulation can be generalized in a straightforward manner to devices moving in more degrees of freedom and with various control elements. Actuation

E. Abraham is with the Department of Aeronautics, Imperial College London, SW7 2AZ, U . K .edo.abraham04@ic.ac.uk

E. C. Kerrigan is with the Department of Aeronautics and the Department of Electrical and Electronic Engineering, Imperial College London, SW7 2AZ, U . K .e.kerrigan@ic.ac.uk

and physical constraints are also easily incorporated in this setting. We will also formulate and use a globally convergent and computationally cheap gradient projection scheme for computing the control commands. We employ a state-of the art interior-point optimization software within a direct collocation method to solve the resulting nonlinear program for comparison and validation.

In Section II, we will discuss the dynamics of a heaving buoy and its state space model derived for control. Section III presents a variational formulation of the optimal control problem and methods to solve it. Finally, in Section IV an example device is used to demonstrate the computational gains from using a projected gradient method. Control feasibility and the improvement that optimal active control delivers over optimal latching control is also presented.

II. System Dynamics

In this article, we consider a semi-submerged cylindrical point absorber constrained to move in heave only; see Fig. 1. A rigid body interacting with an inviscid, incompressible and irrotational fluid flow is assumed. Considering the sea bottom as an inertial reference, the vertical displacement of the buoy from the equilibrium (in the absence of waves) is represented by $\zeta(t)$. Then, the buoy displacement with time t is given as

$$M\ddot{\zeta}(t) = f_c(t) + f_h(t) + f_r(t) + f_{exc}(t), \tag{1}$$

where M is the mass of the body and f_c represents the vertical control force exerted on the buoy. The net hydrostatic restoring force due to buoyancy and gravity is given by f_h and is proportional to the displacement

$$f_h(t) = -C_h\zeta, \tag{2}$$

where the hydrostatic stiffness $C_h := \rho g S$, with ρ being the density of water, g gravitational acceleration and S the cross-sectional area of the buoy. The heave excitation force f_{exc} is the force exerted on the stationary body at equilibrium due to the interaction with the oncoming waves. The radiation forces f_r describe the forces due to the movement of the body itself in the absence of incident waves; changes in the momentum of the surrounding fluid and the resulting radiated waves give rise to net forces on the body. Assuming a linear water-body interaction and using velocity potential theory these forces can be linearly related to the displacement, velocity and acceleration of the buoy in the frequency domain; see [1] and references therein for the derivation of frequency domain transfer functions relating the velocities with radiation and excitation forces for some floating geometries in water.

A time-domain approach models the radiation force using

$$f_r(t) = -\mu_\infty\ddot{\zeta}(t) - \int_{-\infty}^{t} k_r(t-\tau)\dot{\zeta}(\tau)d\tau, \tag{3}$$

also referred to as the Cummins equation [14]. The so-called infinite-frequency added mass μ_∞ represents an instantaneous force response of the fluid after an impulsive movement of the buoy. The convolution integral represents forces due to the transient fluid motion or radiated waves caused by the

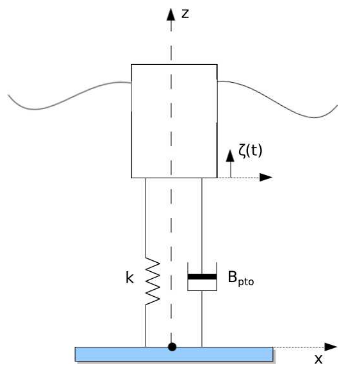

Fig. 1. A schematic of heaving buoy point absorber WEC.

motion of the buoy. The impulse-response of the radiation force $k_r(\cdot)$ can be computed using time-domain simulations via software like WAMIT and ACHIL3D [6]. The equation of motion (1) can now be re-written as:

$$\begin{aligned}(M+\mu_\infty)\ddot{\zeta}(t) + \int_{-\infty}^{t} k_r(t-\tau)\dot{\zeta}(\tau)d\tau \\ +C_h\zeta(t) = f_{ext}(t) + f_c(t).\end{aligned} \tag{4}$$

In a control algorithm, (4) would have to be solved at each time. However, this computation is more efficiently calculated with an approximate state-space model for the convolution integral [15]. Considering the velocity $\dot{\zeta}(t)$ as the input of a linear time-invariant continuous-time system of order m and the integral approximation $y_r(t)$ as the output, we have:

$$\begin{aligned}\dot{z}_r(t) &= A_r z(t) + B_r\dot{\zeta}(t), z_r(0) = 0, \\ y_r(t) &= C_r z_r(t) \approx \textstyle\int_{-\infty}^{t} k_r(t-\tau)\dot{\zeta}(\tau)d\tau,\end{aligned} \tag{5}$$

where the state $z_r(t) \in \mathbb{R}^m$, $A_r \in \mathbb{R}^{m\times m}$, $B_r \in \mathbb{R}^{m\times 1}$ and $C_r \in \mathbb{R}^{1\times m}$. As in [13], we call this the *radiation subsystem*. With a radiation subsystem of order $m = n-2$ identified in (5), the WEC system dynamics can be re-written in state space form as:

$$\begin{aligned}\dot{x}_1(t) &= x_2(t), \\ \dot{x}_2(t) &= \tfrac{1}{M+\mu_\infty}[f_{exc}(t) + f_c(t) - C_r x_{3:n}(t) - C_h x_1(t)], \\ \dot{x}_{3:n}(t) &= A_r x_{3:n}(t) + B_r x_2(t),\end{aligned} \tag{6}$$

where the notation $x_{a:b}$ is to be interpreted as 'elements a to b of the state vector x' and the new state $x := [x_1\ x_2\ \ldots\ x_n]^T = [\zeta\ \dot{\zeta}\ z_r^T]^T \in \mathbb{R}^n$ with the appropriate initial conditions. See [16] and references therein for methods of system identification – we use the time-domain method implemented in the Matlab function `imp2ss` and discussed in this reference. In the following, we assume all states are known. Observers can be designed for the radiation and excitation forces from position, velocity and other sensor information.

III. Optimal Control Problem

The aim here is to examine the optimal control problem to be used within a receding horizon framework. The underlying basis of this method is an iterative, finite-time optimization of the plant model [17]. At any sampling instant, the measured state values are used as initial conditions to calculate an optimal input function or sequence and the associated future state trajectory. Therefore, at the root are an optimal control algorithm to find the input sequence, and an ordinary differential equation (ODE) solver to calculate the state trajectory. Here, we investigate the optimal control problem for maximizing energy extracted from a generic WEC. As in all the discussed literature, we assume that the excitation force is known in the prediction horizon. In practice, this is not true and an estimate would be used.

A. The Optimal Control Problem

Let us consider the WEC of (6) again. Here we assume that power is taken off through a damping force proportional to the velocity (with the constant damping coefficient B_{pto} being controlled proportionally through the input command $u_2(t) \in [0,1]$) and a bounded active forcing element; i.e. $f_c(t) = -B_{pto}u_2(t)x_2(t) + u_1(t)G$, where $u_1 \in [-1,1]$ and $G > 0$ is a (large) constant with a unit of force (N). The equation of motion (6) can then be re-written as:

$$\begin{aligned} \dot{x}_1(t) &= x_2(t), \\ \dot{x}_2(t) &= \tfrac{1}{M+\mu_\infty}[f_{exc}(t) + Gu_1(t) - \\ & \quad B_{pto}u_2(t)x_2(t) - C_r x_{3:n}(t) - Cx_1(t)], \\ \dot{x}_{3:n}(t) &= A_r x_{3:n} + B_r x_2(t), \end{aligned} \tag{7}$$

where $C := (C_h + k)$, k is the stiffness of an external spring system attached to the buoy, $u_1(t) \in [-1,1]$ and $u_2(t) \in [0,1]$. This dynamics is that of a *bilinear system*, i.e. it is linear in the input and linear in the state, but not jointly linear in both. From here on, where convenient, we use the augmented input vector $u(t) := [u_1(t)\ u_2(t)]^T$ and the set $\mathbb{U} := \{u(\cdot) : u_1(t) \in [-1,1]$ and $u_2(t) \in [0,1],\ \forall t \in [t_0,\ t_f]\}$. The objective, at time $t = t_0$, is to maximize the energy E extracted over a future time interval $[t_0,\ t_f]$; we solve the optimal control problem:

$$OCP: \min_{u(\cdot)\in\mathbb{U}} \int_{t_0}^{t_f} \{-B_{pto}u_2(t)x_2^2(t) + Gu_1(t)x_2(t)\}dt. \quad \text{subject to (7) and } x(t_0) = \hat{x} \text{ given.} \tag{8}$$

The dynamic constraint of (7) can be added to the minimization problem using a Lagrange multiplier $\lambda \in \mathbb{R}^n$ as

$$J := -E + \int_{t_0}^{t_f} \lambda^T(t)[f(x(t),u(t),t) - \dot{x}(t)]dt \tag{9}$$

where $f(\cdot)$ is a vector representation of the right hand side of (7) and $x(t)$ the state. The Hamiltonian associated with the minimization of J then becomes [18, Sec. 2.3]:

$$\begin{aligned} H(x,u,\lambda,t) := &-B_{pto}u_2x_2^2 + Gu_1x_2 + \lambda_1x_2 + \frac{\lambda_2}{M+\mu_\infty}\{f_{exc}(t) + \\ & Gu_1 - B_{pto}u_2x_2 - C_r x_{3:n} - Cx_1\} + \\ & \lambda_{3:n}^T(A_r x_{3:n} + B_r x_2). \end{aligned} \tag{10}$$

(t in u, x and λ is dropped for notational convenience).

Pontryagin's minimum principle (PMP) considers the above formulation and derives necessary (and sufficient) conditions for optimality based on the idea that small variations of a locally optimal control u should not decrease the objective function of the minimization problem. We consider an optimal input $u(\cdot) \in \mathbb{U}$ and an arbitrarily small admissible perturbation $\delta u(\cdot)$, i.e. $u(t) + \delta u(t) \in \mathbb{U}, \forall t \in [t_0, t_f]$ and $\|\delta u(t)\|_{L^1} < \varepsilon$, where for $v : [0,\infty) \to \mathbb{R}^m$, $\|v\|_{L^1} := \int_0^\infty \sum_{i=1}^m |v_i(t)|dt$ [19, Sec. 3.4]. The cost function can then be shown to satisfy:

$$\begin{aligned} J(u+\delta u) - J(u) = &\int_{t_0}^{t_f} \{H(x,u+\delta u,\lambda;t) - H(x,u,\lambda;t)\}dt \\ &+ O(\varepsilon), \end{aligned} \tag{11}$$

where ε is a small number and the vector of adjoint variables λ satisfy the set of adjoint differential equations

$$\dot{\lambda}(t) = -\frac{\partial H^T}{\partial x}(x(t),u(t),\lambda(t),t), \tag{12}$$

and the final condition is $\lambda(t_f) = 0$, because the terminal cost is zero. Detailed derivations are available in [19, Ch. 3].

Generally, through the weak form of the PMP, a candidate (locally) optimal control law $u(\cdot)^*$ can be derived from the first order necessary condition $H_u := \partial H(\cdot)/\partial u = 0$ and sufficient conditions are verified using $\partial^2 H(\cdot)/\partial u^2$ or by substituting $u(\cdot)^*$ into the objective function. However, since both the performance measure in (8) and the dynamics (7) are linear in the control input, u does not appear in H_u. Therefore, it does not give us a candidate optimal control. A first order necessary condition for optimality, i.e. for $J(u+\delta u) - J(u)$ in (11) to be non-negative, is then [19, Thm 3.4.2]

$$\begin{aligned} H(x(t),u(t)^*,\lambda(t);t) \le &H(x(t),u(t),\lambda(t);t), \\ &\forall u(t) \in \mathbb{U},\ \forall t \in [t_0,t_f], \end{aligned} \tag{13}$$

where $H(\cdot)$ and $\lambda(\cdot)$ are as defined in (10), and (12), respectively. Simply put, the PMP states that the optimal control, and its corresponding state and co-state trajectories, must minimise the Hamiltonian for all time $t \in [t_0,t_f]$ and for all "neighbouring" admissible inputs.

In problems where the control is bounded, i.e. $\mathbb{U} := \{u(\cdot) : u(t) \in [u_{min},u_{max}], \forall t \in [t_0,t_f]\}$, (13) allows us to show necessary conditions for optimality. Moreover, the system dynamics and the cost function being linear in the input makes the Hamiltonian affine in the control, i.e. it has the form:

$$\begin{aligned} H(x(t),u(t),\lambda(t);t) = &l(x(t),\lambda(t),t) + \sigma(x(t),\lambda(t),t)^T\ u(t) \\ &\forall t \in [t_0,t_f], \end{aligned} \tag{14}$$

where $l(x(t),\lambda(t),t) \in \mathbb{R}$ and $\sigma(x(t),\lambda(t),t) \in \mathbb{R}^m$, $\forall x,\lambda,t$. The necessary condition of (13) then reduces to:

$$\begin{aligned} \sigma(x(t),\lambda(t),t)^T\ u^*(t) \le &\sigma(x(t),\lambda(t),t)^T\ u(t) \\ &\forall u(t) \in \mathbb{U},\ \forall t \in [t_0,t_f]. \end{aligned} \tag{15}$$

This further simplifies to componentwise conditions on the optimal input, namely:

$$u_i^*(t) = \begin{cases} u_{min,i} & \text{if } \sigma_i(x(t),\lambda(t),t) > 0, \\ u_{max,i} & \text{if } \sigma_i(x(t),\lambda(t),t) < 0, \\ \text{undetermined} & \text{if } \sigma_i(x(t),\lambda(t),t) = 0, \end{cases} \quad \text{for } i = 1,\dots,m,\ \forall t \in [t_0,t_f]. \tag{16}$$

It is clear that $\sigma(\cdot) = H_u(\cdot)$. The components $\sigma_i(\cdot)$ are called switching curves; the optimal input components switch from one boundary to the other at the zero crossings of the corresponding function. We say a singular arc occurs if any of the switching functions $\sigma_i(\cdot), i = 1,\ldots m$, vanishes identically on an interval of nonzero measure in $[t_0,t_f]$. In such intervals, (16) does not determine the optimal input — additional conditions from successive differentiation of the switching functions are used to determine the optimal input [18, Ch. 6], [20]. From (10), the switching function vector is given as:

$$\begin{aligned}\sigma(x,\lambda,t) \quad &:= [\tfrac{\partial H}{\partial u_1} \ \ \tfrac{\partial H}{\partial u_2}]^T \\ &= [G(x_2 + \tfrac{\lambda_2}{M+\mu_\infty}) \ \ -B_{pto}x_2(x_2 + \tfrac{\lambda_2}{M+\mu_\infty})]^T, \\ &\forall t \in [t_0,\, t_f].\end{aligned} \tag{17}$$

Although not presented here for the sake of brevity, taking successive time derivatives of the switching functions (17), one can show the absence of singular arcs for the system considered. A proof by contradiction can be used to show a possible optimal singular controller does not satisfy the necessary conditions in [20, Thm 6.2 and Cor. 6.3].

B. Optimal Control Algorithm: a Gradient Projection Scheme

Although we had started Section III-A with the assumption that our control inputs can take a continuum of values in a bounded set, we showed the optimal control inputs take values only on the feasible set boundary. With this in mind and assuming the digital control implementation will be piecewise constant, we solve an approximate finite-dimensional optimization problem. The new problem is approximate in the sense that we are seeking an input in a piecewise continuous and bounded subset of the infinite dimensional original feasible set $\mathbb{U}$ but solve the same objective function as in OCP. We outline the online control synthesis algorithm below.

Assume piecewise constant inputs, i.e. $u(t) = u(t_j) \in \mathbb{R}^m,\ \forall t \in [t_j,t_{j+1}),\ t_{j+1} = t_j + h,\ \forall j \in \{0,1,\ldots,N-1\}$ and $h := \frac{t_f - t_0}{N}$. Let $u_{i,j} = u_i(t_j)$, then our aim is to find an optimal control sequence $\bar{u} = \{u_{1:m,j}\} \in \mathbb{V} \subset \mathbb{R}^{m\times N}$, where $\mathbb{V} = \{\{u_{1:m,j}\} : u_{i,j} \in [u_{min,i}, u_{max,i}] \subset \mathbb{R},\ i = 1,...,m,\ j = 0,1,\ldots,N-1\}$, $u_{min,i}$ and $u_{max,i}$ are the lower and upper bounds, respectively, on the i^{th} control input and $u_{1:m,j}$ is to be interpreted as the input vector at time t_j .

Although more advanced schemes could be used (see Section IV), the method we adopt here is to iteratively improve the input sequence by minimizing the objective function (9) using a variation of the steepest descent method. This method has the nice property that it is globally convergent to stationary points under mild assumptions [21]. The main advantage of our particular scheme is its smaller computational cost; it requires only a single state and adjoint evaluation at each iteration and converges within a small number of iterations.

With a feasible initial choice $\bar{u}^0$, traditional gradient methods like the steepest descent method seek iterates

$$\hat{u}^{k+1} := \bar{u}^k - s^k \nabla J(\bar{u}^k), \tag{18}$$

where s^k is the step size at iteration k. The gradient, $\nabla J(\bar{u}^k) := \frac{dJ}{du}(\bar{u}^k)$, is an $m \times N$ matrix whose components in (19) measure the variation of the cost function with respect to each input and within each sampling interval. From (11) we get:

$$\begin{aligned}\nabla J(\bar{u}^k)_{i,j} \quad &= \textstyle\int_{t_j}^{t_{j+1}} \frac{\partial H^T}{\partial u_i}(x(t),u(t),\lambda(t),t)dt|_{\bar{u}^k}, \\ &= \textstyle\int_{t_j}^{t_{j+1}} \sigma_i(x(t),\lambda(t);t)dt|_{\bar{u}^k},\end{aligned} \tag{19}$$

where $i = 1,\ldots,m$ refers to the input component and $j = 0,\ldots,N-1$ identifies the sampling interval in $[t_0,t_f]$.

The tenet of a projected gradient method (PGM) is that it keeps the iterates feasible. In every iteration, a step in the direction of the anti-gradient is taken and the result in (18) is projected onto the feasible set $\mathbb{V}$,

$$\begin{aligned}\bar{u}^{k+1} \quad &:= \quad P_{\mathbb{V}}(\hat{u}^{k+1}), \\ P_{\mathbb{V}}(\hat{u}) \quad &:= \quad \arg\min_{\bar{v}\in\mathbb{V}} \|\bar{v} - \hat{u}\|.\end{aligned} \tag{20}$$

$$\text{Therefore,} \quad \bar{u}_{i,j}^{k+1} = \begin{cases} u_{max,i} & \text{if } \hat{u}_{i,j}^{k+1} > u_{max,i}, \\ u_{min,i} & \text{if } \hat{u}_{i,j}^{k+1} < u_{min,i}, \\ \hat{u}_{i,j}^{k+1} & \text{otherwise }, \end{cases} \quad \text{for } i = 1,\ldots,m,\ j = 0,\ldots,N-1. \tag{21}$$

Although this projection operation can be computationally demanding with a substantial overhead for a general feasible set, it is easily computed for simple convex sets like the polyhedron (or box) set $\mathbb{V}$ considered here. The projection is a simple element-wise bounding in (21) and, therefore, its computational demand is marginal. To make use of existing PGM results, we make the following technical assumptions:

1) The objective function $J(\cdot;x_0)$ is continuously differentiable and bounded from below on the closed convex set $\mathbb{V}$.
2) The gradient $\nabla J(\cdot;x_0)$ is Lipschitz, i.e. $\exists\, L \geq 0$ such that $\|\nabla J(\bar{u}) - \nabla J(\bar{v})\| \leq L\|\bar{u} - \bar{v}\|$, $\forall \bar{u},\bar{v} \in \mathbb{V}$, where $\|\cdot\|$ can be any p-norm. We assume, of course, that x_0 is bounded and that the state and co-state trajectories stay bounded.

From the definitions of the dynamics and the objective function, it is trivial that the cost $J(\cdot)$ is continuous in the input and bounded from below. Using the standard result that the state and adjoint variables are continuous even under piece-wise continuous (or bang-bang) inputs [18], from (19), the gradient of the cost is continuous with respect to input variations in $\mathbb{V}$. The Lipschitz assumption results from the continuity and boundedness of $\nabla J(\cdot)$ over the compact set $\mathbb{V}$.

With these assumptions, one can show that the projected gradient method converges to a local minimum for various step-size rules [21, Sec. 2.3]. As in the steepest descent method, the limitation of this method is that it generally has poor convergence. Nonetheless, it is shown in [21] that fast (superlinear) convergence can be achieved using a combination of Armijo-type line search schemes and Newton

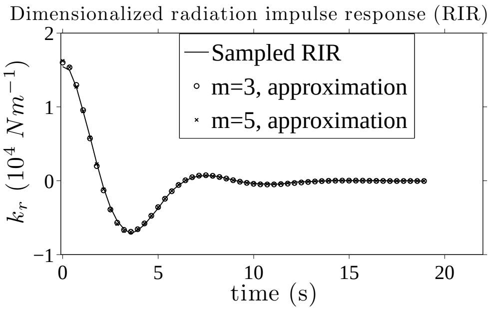

(a)

Fig. 2. (a) A radiation subsystem of order 3 is good enough to approximate the radiation impulse response sufficiently.

and quasi-Newton methods. These, however, are complex algorithms performing line searches and associated function and Hessian evaluations at each iteration and have overheads comparable to complex NLP solvers. For convex problems, fast gradient methods that use a constant step-length with slight modifications can still achieve the best of either linear or quadratic convergence rates [22]. Since the problem considered here is not convex and the aim is to avoid the overhead incurred in performing line searches and associated Hessian and function evaluations at each step, we opt for a constant step-length scheme.

Theorem 1: With the above assumptions satisfied on the closed convex set $\mathbb{V}$, taking a constant step-size $s^k = s$, where $0 < s \leq \frac{2(1-\sigma)}{L}$, $0 < \sigma < 1$, the algorithm in (20) is globally convergent to a local minimum (or stationary point) and the following are valid:

$$J(\vec{u}^k) - J(\vec{u}^{k+1}) \geq \frac{\sigma}{s}\|\vec{u}^k - \vec{u}^{k+1}\|^2, \tag{22a}$$

$$J(\vec{u}^k) - J(\vec{u}^{k+1}) \geq \min\{1, s\}\frac{\sigma}{s}\|\vec{u}^k - P_{\mathbb{V}}\{\vec{u}^k - s\frac{dJ^T}{d\vec{u}}(\vec{u}^k)\}\|^2. \tag{22b}$$

Proof: The global convergence of the algorithm and the conditions in (22a)-(22b) are a standard result and relegated to [21, Sec. 2.3.2] or [23, Thm 4.1]. ■

We have proposed a method that is globally convergent to a local minimum. Although only a sublinear global convergence rate can be guaranteed, the algorithm converges much quicker (at worst, within a few tens of iterations) than what is predicted by the convergence analysis – the reduction in the cost at each iteration in (22b) does not diminish until we get very close to a minimum, in which case we have converged for all practical purposes and the solution can be rounded to the nearest vertex of the polyhedron set $\mathbb{V}$. It should also be noted that the Lipschitz constant L is usually unavailable, and so we cannot determine the range of feasible step sizes s^k a priori. We will, however, demonstrate that choosing an appropriate s^k via offline simulations under various conditions would suffice.

IV. Example Simulations

For the semi-submerged heaving cylinder that we consider, non-dimensionalized impulse response kernels for the radiation and excitation forces from [15] were used. We scale the problem to an appropriate size roughly comparable to the device in [6]; a cylinder of radius $R = 5$ m, and 20 m high with a spring of stiffness $k = 240$ kN/m will be used. From the dimensionalization relation used in [15], we calculate the draught to be 9 m in 42.85 m deep waters. The spring is assumed slack at equilibrium (no wave), and the mass of the device is $M = 707$ t (tonnes) with $\mu_\infty = 0.345 * M \approx 244$ t from the relation in [15] and water density $\rho = 1000$ kg/m^3.

Fig. 2(a) shows that a 3$^{\text{rd}}$ order radiation subsystem is enough to approximate the sampled radiation impulse response; the excitation force is generated using a 6$^{\text{th}}$ order state space model [15]. A JONSWAP spectrum will be used to generate the wave profile.

The projected gradient method was tested to see its convergence properties under different wave conditions. The results were compared to the results from solving a direct transcription of the optimal control problem using state of the art open-source optimization software (IPOPT, version 3.9.2) [24]. Euler, trapezoidal and Hermite-Simpson collocation schemes were used for the IPOPT implementation (see [25, Sec. 4.5]). The explicit Runge-Kutta (4,5) method (Matlab's `ode45`) was used to integrate the dynamics and adjoint dynamics within the PGM implementation. At each iteration of the IPOPT implementation, gradient and Hessian computations of the Lagrangian, as well as a number of line searches are performed (see [21]). On the other hand, the PGM method described in Section III-B requires only a single state and costate evaluation; the gradient computation and the projection onto the feasible input set add only marginal computational cost.

In all the simulations, the control inputs have a sampling period of 0.1s; the states and adjoint states are resolved at a 5 times finer rate. IPOPT was set to use an adaptive barrier parameter update strategy since it resulted in better convergence in simulations. For the PGM, a value for the constant step-size was chosen a posteriori from simulations. A value of $s = \frac{2}{G}$ was found to work sufficiently well under all the wave conditions presented. It can be seen from Figure 3(a) that the PGM converges more quickly than IPOPT to the same local optima. The test was done under different wave conditions, parameter values and WEC initial conditions to confirm similar performances.

A snippet of the device response under the optimal active controller is shown in Figure 3(b). An interesting point to note is that the damper is off (or bypassed) when the active controller is aiding the motion (i.e. when the control input u_1 has the same sign as the velocity $\dot{\zeta}$) and engaged when the active element resists motion. Figure 3(c) compares the active optimal control developed with optimal command latching and the case with no control. The active controller increases extracted power significantly. Unlike latching control, the active method widens the bandwidth of the WEC in both directions around the natural frequency of the WEC; latching is effective at frequencies lower than that of the buoy. Although the device has a natural period of 6s, the parameters B_{pto} and G were optimized for a wave of typical period 8s.

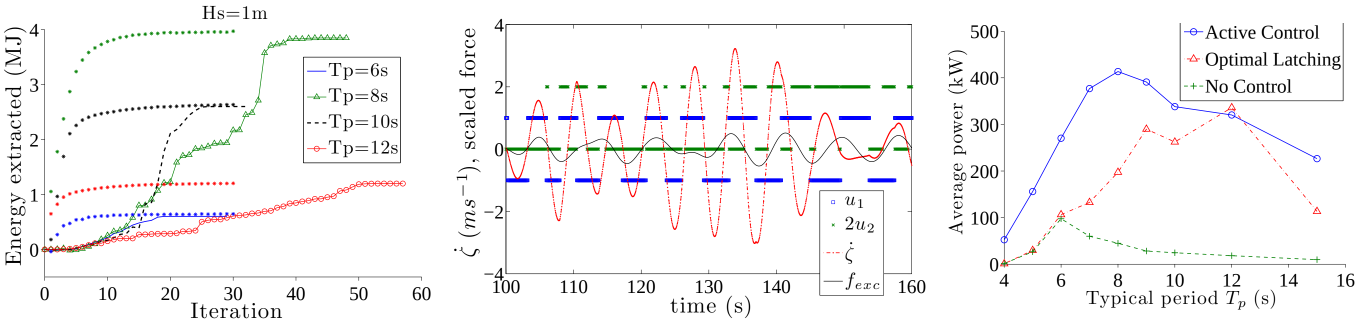

(a) (b) (c)

Fig. 3. (a) Convergence of the PGM algorithm (dotted, left) against that of a direct transcription solution using IPOPT (with legend) over a 50 s prediction horizon for waves of different typical period (T_p) (b) A plot of the device velocity against control commands and normalized excitation force under optimal active control (c) Average absorbed power against typical wave period with the different control methods, $B_{pto} \approx 280$ kN·s/m ($B_{pto} \approx 95$ kN·s/m for latching control), $G = M + \mu_\infty$, $T_p = 8$ s, $H_s = 2$m.

V. Conclusion

In this paper, an optimal active control method for a receding horizon control strategy was considered. A state space model of a generic point absorber, whose power take-off includes a linear damper and an active element, was formulated and used. By considering a variational formulation of the optimal control problem, the solution can be shown to be of bang-bang type when constraints are imposed only on the control forces.

A computationally inexpensive and globally convergent numerical scheme was developed for solving the power maximization problem. A variation of the projected gradient method (PGM) was exploited and shown to converge in a small number of iterations under various wave conditions. Its performance has been compared to solving a directly collocated version of the problem using a state of the art interior point solver, IPOPT. As the PGM requires only a single state and costate evaluation at each iteration, it was shown to be far less computationally demanding compared to a general NLP solver. Time-domain simulations have also been used to evaluate the performance of the controller developed; it has a wider bandwidth and a larger power yield than optimal latching when large enough actuation forces are used.

References

[1] J. Falnes, *Ocean waves and oscillating systems: linear interaction including wave-energy extraction*. Cambridge University Press, 2002.

[2] ——, "Optimum control of oscillation of wave-energy converters." *International Journal of Offshore and Polar Engineering*, vol. 12, no. 2, pp. 147–154, 2002.

[3] K. Budal, J. Falnes, L. C. Iversen, P. M. Lillebekken, G. Oltedal, T. Hals, T. Onshus, and A. S. Høy, "The norwegian wave-power buoy project," in *The Second International Symposium on Wave Energy Utillization, Trondheim*, 1982.

[4] R. E. Hoskin and N. K. Nichols, "Latching control of a point absorber." in *Proc. 3rd International Symposium on Wave, Tidal, OTEC, and Small Scale Hydro Energy*, 1986, pp. 317–330.

[5] A. Babarit, G. Duclos, and A. H. Clément, "Comparison of latching control strategies for a heaving wave energy device in random sea," *Applied Ocean Research*, vol. 26, no. 5, pp. 227–238, 2004.

[6] A. Babarit and A. H. Clément, "Optimal latching control of a wave energy device in regular and irregular waves," *Applied Ocean Research*, vol. 28, no. 2, pp. 77–91, 2006.

[7] A. F. O. Falcão, "Phase control through load control of oscillating-body wave energy converters with hydraulic PTO system," *Ocean Engineering*, vol. 35, no. 3-4, pp. 358–366, 2008.

[8] U. A. Korde, "Phase control of floating bodies from an on-board reference," *Applied Ocean research*, vol. 23, no. 5, pp. 251–262, 2001.

[9] J. J. Cândido and P. A. P. S. Justino, "Modelling, control and pontryagin maximum principle for a two-body wave energy device," *Renewable Energy*, 2010.

[10] J. Falnes, "Radiation impedance matrix and optimum power absorption for interacting oscillators in surface waves," *Applied Ocean Research*, vol. 2, no. 2, pp. 75–80, 1980.

[11] A. Babarit, M. Guglielmi, and A. H. Clément, "Declutching control of a wave energy converter," *Ocean Engineering*, vol. 36, no. 12, pp. 1015–1024, 2009.

[12] J. Hals, J. Falnes, and T. Moan, "Constrained optimal control of a heaving buoy wave-energy converter," *Journal of Offshore Mechanics and Arctic Engineering*, vol. 133, p. 011401, 2011.

[13] J. A. M. Cretel, G. Lightbody, G. P. Thomas, and A. W. Lewis, "Maximisation of energy capture by a wave-energy point absorber using model predictive control," in *Proc. IFAC World Congress on Automatic Control, Milano, Italy*, 2011.

[14] W. E. Cummins, "The impulse response function and ship motions," Hydrodynamics Laboratory Research and Development Report, Tech. Rep. Report number 1661, 1962.

[15] Z. Yu and J. Falnes, "State-space modelling of a vertical cylinder in heave," *Applied Ocean Research*, vol. 17, no. 5, pp. 265–275, 1995.

[16] R. Taghipour, T. Perez, and T. Moan, "Hybrid frequency-time domain models for dynamic response analysis of marine structures," *Ocean Engineering*, vol. 35, no. 7, pp. 685–705, 2008.

[17] J. M. Maciejowski, *Predictive control: with constraints*. Pearson Education, 2002.

[18] A. E. Bryson and Y. C. Ho, *Applied optimal control: optimization, estimation, and control*. Hemisphere Publications, 1975.

[19] J. L. Speyer and D. H. Jacobson, *Primer on optimal control theory*. Society for Industrial and Applied Mathematics (SIAM), 2010.

[20] A. J. Krener, "The high order maximal principle and its application to singular extremals," *SIAM Journal on Control and Optimization*, vol. 15, no. 2, pp. 256–293, 1977.

[21] D. P. Bertsekas, *Nonlinear programming*. Athena Scientific Belmont, Massachusetts, 1999.

[22] S. Richter, C. N. Jones, and M. Morari, "Real-time input-constrained MPC using fast gradient methods," in *Proc. IEEE Conference on Decision and Control*, Shanghai, China, December 2009, pp. 7387–7393.

[23] Z. Q. Luo and P. Tseng, "On the linear convergence of descent methods for convex essentially smooth minimization," *SIAM J. Control Optim*, vol. 30, no. 2, pp. 408–425, 1992.

[24] A. Wächter and L. T. Biegler, "On the implementation of an interior-point filter line-search algorithm for large-scale nonlinear programming," *Mathematical Programming*, vol. 106, no. 1, pp. 25–57, 2006.

[25] J. T. Betts, *Practical methods for optimal control and estimation using nonlinear programming*. Cambridge University Press, 2010.